Chapter 5
Heat Transfer to Structural Elements

Kevin LaMalva, Cristian Maluk, Ann Jeffers, and Allan Jowsey

This chapter covers the following topics:

- Fundamentals of heat transfer and description of basic engineering concepts for describing the thermal boundary conditions for solid elements (e.g., structural elements) during fire.
- Formulation of heat transfer from the fire to structural elements in terms of heat fluxes.
- The thermal properties of materials used in a heat transfer analysis.
- Special design considerations associated with nontypical heating conditions and nonstandard materials.

K. LaMalva (✉)
Warringtonfire, Boston, MA, USA
e-mail: kevin.lamalva@warringtonfire.com

C. Maluk
School of Civil Engineering, University of Queensland, Brisbane, QLD, Australia
e-mail: c.maluk@uq.edu.au

A. Jeffers
Civil and Environmental Engineering Department, University of Michigan, Ann Arbor, MI, USA
e-mail: jffrs@umich.edu

A. Jowsey
PFP Specialists, Sudbury, UK
e-mail: allan.jowsey@pfpspecialists.co.uk

K. LaMalva, D. Hopkin (eds.), *International Handbook of Structural Fire Engineering*, The Society of Fire Protection Engineers Series,
https://doi.org/10.1007/978-3-030-77123-2_5

5.1 Fundamentals of Heat Transfer

This section covers the fundamentals of heat transfer and describes basic engineering concepts for describing the thermal boundary conditions for solid elements (e.g., structural elements) during fire.

5.1.1 Summary of Heat Transfer

When analyzing the heat transfer from the fire to a structural element the problem needs to be formulated in terms of heat fluxes. While temperature of the solid phase results from solving the energy conservation equations, all quantities to be balanced are energies. The correlation between temperature and heat flux can be linear, but this is only under the assumption that an overall constant heat transfer coefficient can be established in space and time. An important aspect, many times overlooked, is the need to make sure that the thermal boundary conditions are properly represented.

The thermal boundary conditions at the surface of the solid are defined by means of the equation below:

$$\dot{q}''_{Tot} = -k\frac{\partial T}{\partial x}\bigg|_{x=0}$$

where k is the thermal conductivity of the solid material.

In this section some basic heat transfer concepts are reviewed simply to extract the relevant parameters that will be used in later sections for discussion. These concepts are not novel and can be found in any heat transfer book. Heat is transferred from gases to solid surfaces via radiation and convection resulting in a total heat flux, $\dot{q}''_{\mathrm{Tot}}$, where

$$\dot{q}''_{\mathrm{Tot}} = \dot{q}''_{rad} + \dot{q}''_{con}$$

where $\dot{q}''_{\mathrm{rad}}$ is the heat transfer via radiation and $\dot{q}''_{\mathrm{con}}$ is the heat transferred via convection. For simplicity, within the scope of this chapter, the problem will only be examined in the direction of the principal heat flux, hence considered to be a one-dimensional problem and with the thermal boundary condition of the solid element (i.e., structural element) defined as

$$\dot{q}''_{\mathrm{Tot}} = -k_i\frac{\partial T}{\partial x}\bigg|_{x=0}$$

which is a generic version of the former equation, and where the thermal conductivity (k_i) is a property of the solid and the gradient of temperature is taken at the surface. In other words, all the heat arriving at the surface of the solid is conducted

into the solid. If there are multiple layers then at each interface the following boundary condition should apply:

$$-k_i \frac{\partial T}{\partial x} = -k_s \frac{\partial T}{\partial x}$$

where the gradients correspond to each side of the interface and the subindex "*s*" is a generic way to represent the next layer of solid. Once the thermal boundary conditions are defined, the energy equation can be solved for each material involved. In the case where two layers of solid are involved ("i" and "s"), then the energy equations take the following form:

$$\rho_i Cp_i \frac{\partial T}{\partial t} = \frac{\partial}{\partial x}\left(k_i \frac{\partial T}{\partial x}\right)$$

and

$$\rho_s Cp_s \frac{\partial T}{\partial t} = \frac{\partial}{\partial x}\left(k_s \frac{\partial T}{\partial x}\right)$$

The solution of the energy conservation equations yields the temperature evolution of the material in space and time. The equations above could be repeated for as many layers as necessary. If the geometry or the fire exposure is complex, then the problem needs to be resolved in two or even three dimensions. If the properties vary with temperature then, as the temperature increases, these properties need to evolve with the local temperature. Variable properties thus require a numerical solution. If a simple analytical solution is to be obtained, then adequate global properties need to be defined. It is important to note that whatever the solution methodology adopted, the temperature of the structure is the result of the resolution of the two equations above using thermal boundary conditions such as those formerly shown. To obtain the numerical solution it is necessary to input material properties for the different layers ("i" and "s"). The material properties required are all a function of temperature and are as follows:

$$\rho_i, Cp_i, k_i \text{ and } \rho_s, Cp_s, k_s$$

where (ρ_i, ρ_s), (Cp_i, Cp_s), and (k_i, k_s) are the densities, specific heat capacity, and thermal conductivity for each layer, respectively.

An assessment of the role of detailed boundary conditions is shown above. Structural performance is an unavoidable result of the real evolution of the in-depth temperature of a structural element in space and time. To define the performance of a structural system in fire it is necessary to establish the correct thermal boundary condition. The evolution of this boundary condition will determine internal temperature distributions and thus structural behavior.

5.1.2 Thermal Boundary Conditions

Fire exposures to structures produce thermal boundary conditions that are most commonly expressed as combined convection and radiation at the surface, as given in the equation above. Specifically, for a solid that is immersed in an optically thick gas with uniform temperature T_g (e.g., as would be the case of a structural element in a furnace), the net heat flux is given as

$$\dot{q}''_{\text{Tot}} = \varepsilon\sigma\left(\overline{T}_g^4 - \overline{T}_s^4\right) + h\left(T_g - T_s\right)$$

where ε = emissivity, σ = Stefan-Boltzmann constant (5.67×10^{-8} W m^{-2} K^{-4}), h = convection heat transfer coefficient, and T_s = surface temperature of the solid. Note that the temperatures needed for the radiative heat flux (i.e., $\overline{T}_g$ and $\overline{T}_s$) must be expressed in units of Kelvin, whereas the temperatures for the convective heat flux (i.e., T_g and T_s) may be given in Celsius.

The equation below is often used to represent heat transfer under standard fire exposure, where the gas temperature T_g follows the ISO 834 [1] standard time-temperature relationship:

$$T_g(t) = 20 + 345\,log\left(\frac{8t}{60} + 1\right)$$

Note that time t is in seconds and temperature T_g is in °C.

In structural fire engineering, the post-flashover fire exposure in a building is often treated the same as the furnace exposure. In other words, the former equation is used to represent the net heat flux at the structure's surface. The gas temperature can be determined from references such as Eurocode 1 [2] or SFPE S.01 [3]. These references provide parametric time-temperature relationships for the fire based on factors such as the fuel load density, thermal properties of the compartment linings, and ventilation conditions in the room. One salient feature of the Eurocode and SFPE fire models is that they include a cooling phase, whereas the standard fire exposure does not.

Another type of heating scenario that is common in structural fire engineering is the heating of materials by radiant panels or heaters, as would be the case, for example, in a cone calorimeter test. In this case, the engineer would likely know the radiant heat flux $\dot{q}''_{\text{inc}}$ produced by the panel. The boundary condition at the solid's surface is then expressed as

$$\dot{q}''_{Tot} = \varepsilon\left(\dot{q}''_{inc} - \sigma\overline{T}_s^4\right) + h\left(T_g - T_s\right)$$

Note that the equation above separates the radiant heat flux from the gas temperature, whereas the former equation presumes that the radiation temperature and convection temperature are equal to one another. It follows that $\dot{q}''_{\text{inc}} = \sigma\overline{T}_r^4$,

where $\overline{T}_r$ is the blackbody radiation temperature (in Kelvin). Thus, the equation above can be expressed as

$$\dot{q}''_{\text{Tot}} = \varepsilon\sigma\left(\overline{T}_r^4 - \overline{T}_s^4\right) + h\left(T_g - T_s\right)$$

An important point to mention is that equations above are nonlinear in temperature, whereas most software for heat transfer analysis use linear equation solvers that solve for temperature in the governing differential equation. As a result, the radiation term is linearized as follows:

$$\dot{q}''_{rad} = h_r\left(\overline{T}_r - \overline{T}_s\right)$$

where

$$h_r = \varepsilon\sigma\left(\overline{T}_r^2 + \overline{T}_s^2\right)\left(\overline{T}_r + \overline{T}_s\right)$$

The assumed form of the thermal boundary conditions drives the selection of instrumentation in structural fire experiments. In furnace tests, for example, it is common to have a measurement of the gas temperature T_g, which is determined using thermocouples. However, it is generally accepted that gas temperature is inadequate for measuring the amount of heat that the structure absorbs by radiation, and so some researchers have advocated for the introduction of plate thermometers in structural fire experiments to measure a property called *adiabatic surface temperature*. Adiabatic surface temperature T_{AST} is defined as the temperature of a perfectly insulated surface. Wickström [4] shows that T_{AST} is a single parameter that will allow the analyst to uniquely account for radiation and gas temperatures (i.e., T_r and T_g, respectively) that are not the same. In particular

$$T_{\text{AST}} = \frac{h_r\overline{T}_r + hT_g}{h_r + h}$$

One important thing to note is that, in this case, h_r is dependent on T_{AST}, so the equation above is not explicit. Nevertheless, the thermal boundary condition may be expressed in the following manner:

$$\dot{q}''_{\text{Tot}} = \varepsilon\sigma\left(\overline{T}_{\text{AST}}^4 - \overline{T}_s^4\right) + h(T_{\text{AST}} - T_s)$$

Other methods exist for measuring the heat flux to a fire-exposed surface, although the methods have some limitations. One approach, for example, uses a water-cooled heat flux gauge to measure the heat flux incident on a surface. For a heat flux $\dot{q}''_f$ measured by the heat flux gauge, the net heat flux at the surface is as follows [5]:

$$\dot{q}''_{\text{Tot}} = \dot{q}''_f - \varepsilon\sigma\left(\overline{T}_s^4 - \overline{T}_g^4\right) - h\left(T_s - T_g\right)$$

5.1.3 Biot Number

The nature of temperature gradients can be defined by the Biot number, *Bi*. The Biot number provides a simple representation of the relationship between the temperature gradients in the gas phase and the temperature gradients in the solid phase:

$$Bi = \frac{h_T d}{k}$$

For extreme values of the Biot number, very large or very small, the temperature gradients in the solid phase are very insensitive to gradients in the gas phase. Therefore, for extreme values of the Biot number, the gas phase and temperature of the solid phase at the exposed surface can be treated with a very simple approximation. Intermediate-range values of the Biot numbers will require precise treatment and most simplifying assumptions will lead to major errors.

Figure 5.1 provides a simple schematic showing the influence of the Biot number in a one-dimensional heat transfer—evidencing the scope for potential simplifications of the heat transfer problem. If the Biot number is close to one (case (b) in Fig. 5.1) temperature gradients in the gas and solid phases are large and therefore equations used to define the thermal boundary conditions will need to be fully resolved, and hence no simplifications are possible. If the Biot number is much greater than one (case (c) in Fig. 5.1) the temperature differences in the gas phase are much smaller than those in the solid phase and it can be assumed that surface and gas temperatures are almost the same. This simplification is very important when modeling furnace tests because it enables the designer to ignore the complex

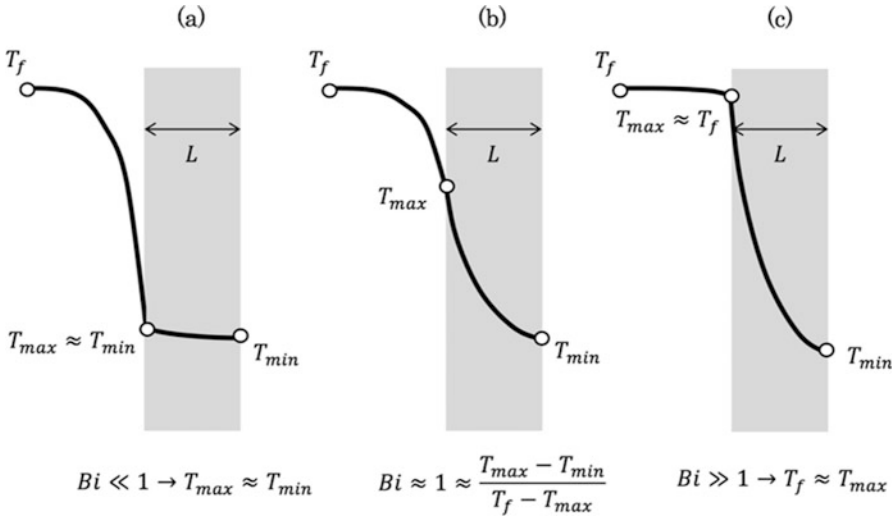

Fig. 5.1 Schematic of the typical temperature distributions for values of the Biot number [(**a**) Biot number much smaller than one (**b**) Biot number close to one (**c**) Biot number much greater than one] [6]

boundary condition imposed by the furnace and simply impose the monitored gas temperature at the surface of the solid. Finally, if the Biot number is much smaller than 1 (case (a) in Fig. 5.1) then the temperature differences in the solid phase are much smaller than those in the gas phase; therefore, temperature gradients in the solid phase can be ignored and a single temperature can be assumed for the solid. Heat conduction within the solid can be approximated by the boundary conditions and the equations used to define the thermal boundary conditions lead to a single temperature solution.

The representation of the thermal response of a structural element by means of a single temperature is therefore only valid if $Bi << 1$. This simplification is called a "lumped capacitance formulation" and while it does not resolve spatial temperature distributions it still requires an adequate definition of the heat transfer between the source of heat (e.g., furnace or "real" fire) and the solid. An important observation is that for materials with Biot numbers much smaller than 1, the thermal energy is rapidly diffused through the integrity of the material, so if the density was to be high, then the lumped solid will lag significantly when compared to the gas-phase temperature. Heat transfer is therefore dominated by the temperature difference between the solid and the gas phase, and errors in the definition of the heat transfer coefficient become less relevant.

It is common for studies attempting to understand the behavior of structures in fire to make use of constant heat transfer coefficients; this will be appropriate for materials with a $Bi << 1$. Nevertheless, there is also significant inconsistencies in the numbers quoted and furnace heat transfer coefficients are many times extrapolated to natural fire coefficients. These values are not necessarily the same, in particular if radiation and convection are to be amalgamated into a single heat transfer coefficient.

Given the importance of the Biot number in the characteristics of the temperature gradients, it is important to estimate the thickness of a material that leads to a $Bi = 1$. Samples that are much thicker will allow approximating the surface temperature to that of the gas phase. Samples that are much thinner will allow to "lump" the solid phase into a single temperature.

Table 5.1 shows typical thermal properties for different construction materials and the characteristic thickness (L) that will result in a Biot number of unity. As can be seen for high-thermal-conductivity materials like aluminum or steel, sections a few millimeters thick can be lumped without any major error. In a similar manner very-low-thermal-conductivity materials like plasterboard or expanded polystyrene (EPS) would allow for the assumption that the surface temperature of the solid is that of the gas phase. In contrast, concrete has a Biot of unity for a thickness of 50 mm that is in between typical concrete cover thicknesses and the overall thickness of the sample. The boundary condition cannot be simplified because the thermal gradients are fully defined by $\dot{q}''_{\mathrm{Tot}}$.

The Biot number can be used to establish if it is necessary to conduct a transient thermomechanical analysis as well as to determine the level of precision necessary when treating the thermal boundary conditions. The following conclusions can be drawn:

Table 5.1 Typical thermal properties for different construction materials

Material	Density (ρ, kg/m^3)	Thermal conductivity (k, W/mK)	Specific heat (Cp, J/kg K)	Thermal diffusivity (α, m^2/s)	*"L"* for $Bi = 1$ (mm)
Aluminum	2400	237	900	1.10E-04	5300
Steel	7800	40	466	1.10E-05	900
Concrete	2000	2.5	880	1.42E-06	50
Plasterboard	800	0.17	1100	1.93E-07	4
Expanded polystyrene (EPS)	20	0.003	1300	1.15E-07	0.1

- The Biot number is a simple nondimensional parameter that combines material characteristics and thermal boundary condition allowing to establish the sensitivity of structural behavior to the precision of the boundary conditions as well as to the transient behavior.
- The Biot number is an effective method to classify different forms of thermally induced structural behavior. The higher the Biot number the lesser transient effects and the more effective the steady-state modeling of a structure to define the worst-case conditions. The lower the Biot number the more important to model transient behavior.
- For the particular case studied, the greater the Biot number the less significant the effect of a fire on structural deformations.

5.2 Heat Transfer Analysis

The heat transfer analysis from the fire to structural elements is formulated in terms of heat fluxes. While temperature of the solid phase results from solving the energy conservation equations, all quantities to be balanced are heat fluxes. For simplicity, commonly the heat transfer analysis is only examined in the direction of the principal heat flux, hence considered to be a one-dimensional problem. This section describes a range of engineering methods and tools for the practical analysis of heat transfer in structural elements.

5.2.1 Lumped Mass Method

As discussed in Sect. 5.1.3, a lumped capacitance (or lumped mass) method is appropriate if $Bi << 1$. The lumped mass method is a step-by-step (i.e., quasi-steady) energy-balance calculation technique that simulates "0-D" heat transfer (i.e., heat transfer with no directionality). Essentially, this method assumes a uniform temperature of a given cross section at any point. Due to its high thermal

conductivity, this method lends itself well to unprotected steel. However, this method would not capture possible longitudinal heat sink effects [7].

Considering an unprotected steel member, the equation below solves for the change in temperature of the steel due to fire exposure over a given time step [8]:

$$\Delta T_s = \left(\frac{F}{V}\right)\left(\frac{1}{\rho_s c_s}\right)\left\{h_c\left(T_f - T_s\right) + \sigma\varepsilon\left(T_f^4 - T_s^4\right)\right\}\Delta t$$

ΔT_s is the change in steel temperature over the time step (K), Δt is the time step (s), F is the surface area of unit length of the member (m^2), V is the volume of steel in unit length of the member (m^3), ρ_s is the density of steel (kg/m^3), c_s is the specific heat of steel (J/kg K), h_c is the convective heat transfer coefficient (W/m^2 K), σ is the Stefan-Boltzmann constant ($56.7 \times 10^{-12} kW/m^2K^4$), ε is the resultant emissivity, T_f (K) is the temperature of the fire environment, and T_s is the steel temperature (K). The convective heat transfer coefficient is recommended to be taken as 25 W/m^2K. Emissivity of the radiating fire gases is recommended to be taken as 1.0 [9]. Thus, the incident radiation is calculated as the blackbody radiation temperature equal to the gas temperature.

The equation above accounts for the geometry of the member (e.g., W-shape beam). Importantly, the F/V ratio represents the influence of the heated perimeter compared to the area of the section. Members with a high F/V ratio would heat up more quickly than comparable members with lower ratios. This effect is evident in many fire-resistant listings, which allow for less protective insulation for more massive members (with a lower F/V ratio). It is recommended that the time step be 30 s or less, and the F/V ratio be at least 10 m^{-1} [10]. Otherwise, the equation may not be valid for the application.

When analyzing structural members with a high thermal capacitance (e.g., concrete members) or steel members with applied protective insulation, the lumped mass method is less suitable. In these cases, the use of a finite element or finite difference model would be significantly more accurate. Nonetheless, if the designer deems this method as conservative, the equation above could be applied directly (e.g., concrete member), or adapted as follows for a steel member with protective insulation [8].

$$\Delta T_s = \left(\frac{F}{V}\right)\left(\frac{k_i}{d_i \rho_s c_s}\right)\left\{\frac{\rho_s c_s}{\rho_s c_s + \frac{\left(F/V\right) d_i \rho_i c_i}{2}}\right\}\left(T_f - T_s\right)\Delta t$$

The equation above does not include heat transfer coefficients, for it is assumed that the external surface of the protective insulation is at the same temperature as the fire environment. It is also assumed that the internal temperature of the protective insulation equals the steel temperature. c_i is the specific heat of the protective insulation (J/kgK), ρ_i is the density of the protective insulation (kg/m^3), k_i is the thermal conductivity of the protective insulation (W/mK), and d_i is the thickness of

the protective insulation (m). For the equation above, it is assumed that the temperature gradient in the insulation is linear. For a steel member with protective insulation, this approximation improves with decreasing insulation thickness.

When using the equation above, the temperature dependence of the protective insulation's thermal properties may be represented by updating the parameter values with each increment of time. However, this exercise would require significant judgment/approximation since this method does not solve for the temperature history of the protective insulation itself. Accordingly, for protective insulation materials that exhibit a strong dependence of its thermal properties on temperature (e.g., gypsum-based material that undergoes an endothermic calcination process during heating), the use of a finite element or finite difference model would be significantly more accurate.

As mentioned above, the lumped mass method does not capture possible longitudinal heat sink effects (e.g., steel girder connection to a heavy column as illustrated in Fig. 5.2). Hence, this method would only provide output on the heating of the section at a significant distance away from heat sinks (e.g., at the girder mid-span). Also, the vertical heat sink effect of a concrete slab and its convective/radiative cooling from its top surface would not be accounted for using this method (as illustrated in Fig. 5.3). These limitations of the method may lead to significant overestimation of the section's temperature history.

5.2.2 Finite Difference Method

A frequent problem in conduction heat transfer involves ascertaining a solution to a transient heat transfer assessment associated with a complex geometry. This is often coupled with the desire to incorporate temperature-dependent material properties which make the application of simplified analytical techniques such as lumped mass not the most appropriate option. Instead, a numerical solution is likely to be a more efficient design tool.

The finite difference method is a numerical technique to solve differential equations by approximating them with difference equations in which finite differences approximate the derivatives. It involves discretization of the geometry of interest into small segments using a series of nodes which are connected by lines to form a grid or mesh. This approach will therefore approximate the geometry with the result being a more refined mesh (smaller grids) that will provide increased accuracy but potentially more computational time. In contrast to an analytical solution which allows for temperature determination at any point within a medium, finite difference will only allow determination of temperature at discrete locations aligned with the nodal positions comprising the mesh.

More than one method exists for obtaining numerical approximations to the solutions of the time-dependent ordinary and partial differential equations. Both explicit and implicit methods are approaches used in numerical analysis of such applications. Explicit methods calculate the state of a system at a later time from the

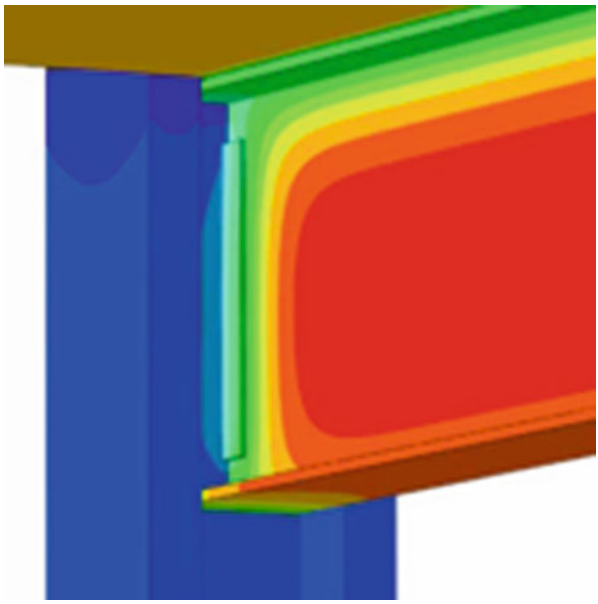

Fig. 5.2 Steel girder connected to heavy column (thermal response)

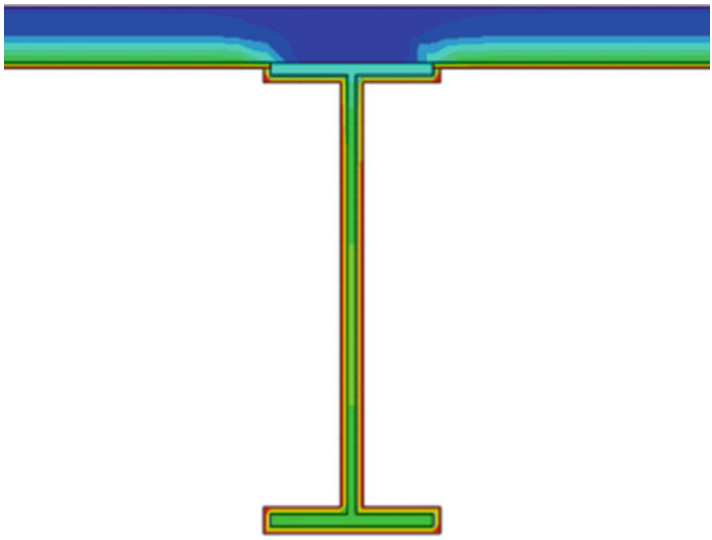

Fig. 5.3 Protected steel girder below a concrete slab (thermal response)

state of the system at the current time, while implicit methods find a solution by solving an equation involving both the current state of the system and the later one. Explicit methods often require impractically small time steps to keep the error associated with the calculation within a reasonable limit (numerical stability). Implicit methods typically take less computational time as they can take advantage

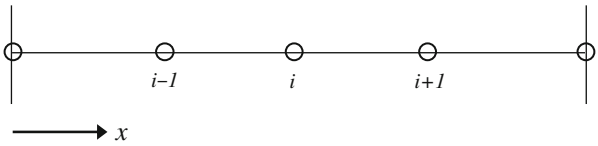

Fig. 5.4 Schematic of a simplified finite difference grid

of larger time steps. Depending on the type of problem to be solved it may be that either an explicit or an implicit approach may be the best.

The finite different method typically uses a Taylor series expansion to reformulate the partial differential equation, resulting in a set of algebraic equations. Consider the basic equation describing heat conduction within a solid:

$$\rho c \frac{\partial \dot{T}}{\partial t} = \frac{\partial}{\partial x}\left(k_1 \frac{\partial T}{\partial x}\right) + \frac{\partial}{\partial y}\left(k_2 \frac{\partial T}{\partial y}\right) + \frac{\partial}{\partial z}\left(k_3 \frac{\partial T}{\partial z}\right) + \dot{q_i'''}$$

where q_i''' is the rate of change of thermal energy stored per unit volume.

In relation to Fig. 5.4, the explicit finite difference form of this for transient heat conduction with no internal heat generation is given as

$$C_i \frac{\left(T_i' - T_i\right)}{\Delta t} = \frac{\frac{k_m(T_{i+1} - T_i)}{\Delta x} - \frac{k_n(T_i - T_{i-1})}{\Delta x}}{\Delta x}$$

where

T_i

the temperature at node i at time t.

T_i'

the temperature at node i after time step, Δt.

$k_m = \frac{1}{2}(k_{i+1} + k_i)$

$k_n = \frac{1}{2}(k_i + k_{i-1})$

$C_i = \rho_i c_p \Delta x$

Alternatively, an implicit formulation can be applied in the form of

$$C_i \frac{\left(T_i' - T_i\right)}{\Delta t} = \frac{\frac{k_m\left(T_{i+1}' - T_i'\right)}{\Delta x} - \frac{k_n\left(T_i' - T_{i+1}'\right)}{\Delta x}}{\Delta x}$$

The advantage of this approach is that it is numerically stable for any time step or grid size. The disadvantage is that all of the equations are coupled as the right-hand side of the equation including nodal temperatures at the end of the time step. Therefore all the equations must be solved simultaneously.

For more complex geometry including 2D or 3D problems, the finite difference equation for a node may also be obtained by applying conservation of energy to a

control volume about the nodal region. This method is often referred to as a heat balance or energy balance approach.

Commercially available software exists to perform finite difference heat transfer calculations.

5.2.3 *Finite Element Method*

Finite element methods (FEM) are efficient numerical methods for solving problems of engineering. Typical applications include structural analysis, heat transfer, fluid flow, mass transport, etc. Similar to the finite difference method, the finite element method can be applied to problems in transient conduction heat transfer associated with a complex geometry.

The finite element method consists of discretizing a geometry into a mesh consisting of nodes and "finite" elements as shown in Fig. 5.5. It is typically possible to generate results either at nodal points or from within elements.

The primary difference in comparison to finite difference methods is that it uses an exact governing equation. Finite element formulations typically use a polynomial fit of the temperature profile within an element to solve the equation. This approach will generally be more accurate for a coarser grid than a finite difference method.

The fundamental equations are outside the scope of this book, but other industry references are available that can explain in further detail. From a high-level perspective, a resulting set of equations are assembled into a matrix in the form of:

$$[C]\{\dot{T}\} + [K]\{T\} = \{Q\}$$

Where

C

is the capacitance matrix, accounting for ρc product associated with each element.

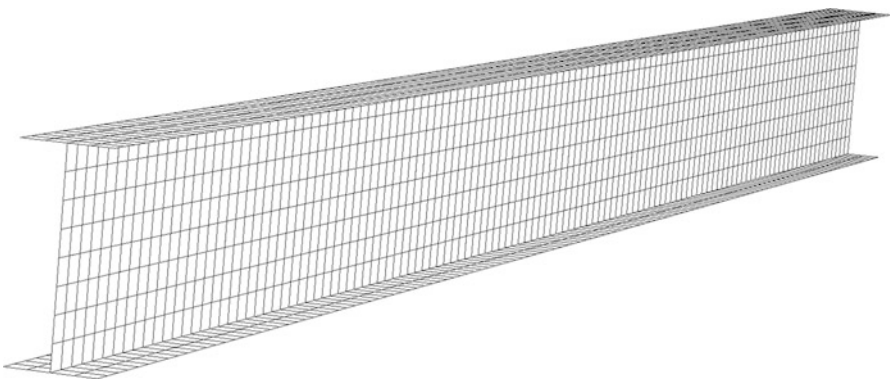

Fig. 5.5 Schematic of a finite element mesh for a beam modeled using shell elements

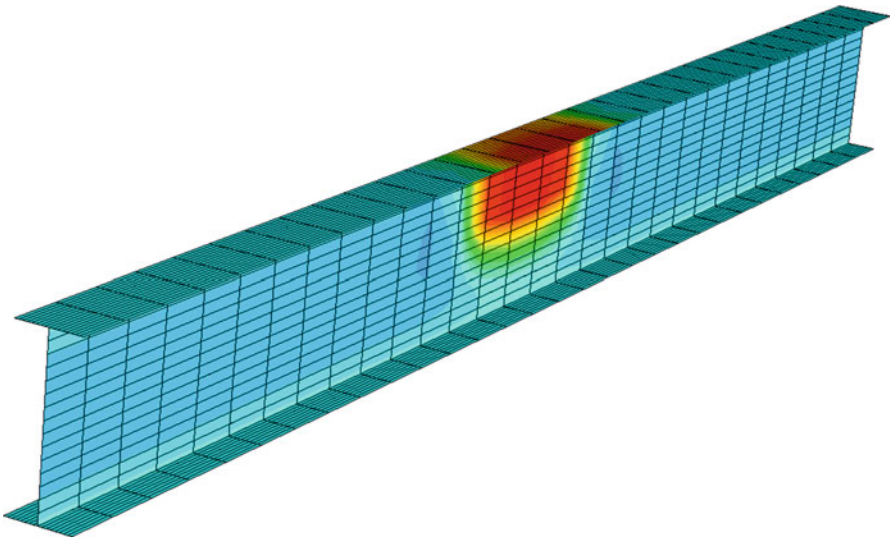

Fig. 5.6 Typical example of a FEM heat transfer assessment

K
is the conductivity matrix, accounting for conductivity of the element.
T
is a vector (column matrix), which represents temperature at each node.
Q
is a vector (column matrix), which represents heat generation at each node.

Determination of the temperature profile within an object requires solving the matrix-based solutions. Commercially available software exists for this purpose. An example of a finite element method heat transfer application associated with temperature contours of a structural arrangement is shown in Fig. 5.6.

5.2.4 Example Problems

Example problems for heat transfer analyses can be found throughout various heat transfer textbooks (e.g., Introduction to Heat Transfer [11]). More specific to structural fire engineering, the SFPE S.02 standard [12] provides the following 16 example problems in its Annex A:

- Lumped Mass Subjected to Standard Fire.
  - *Simplified (0-D) furnace test thermal prediction.*
- Lumped Mass Subjected to Incident Flux.
  - *Simplified (0-D) general-purpose thermal prediction.*

- 1-D Heat Transfer with Cooling by Convection
  - *Unexposed surface thermal prediction.*
- 1-D Axisymmetric Heat Transfer by Convection
  - *Circular cross-section thermal prediction (convection only).*
- Axisymmetric Heat Transfer by Convection and Radiation.
  - *Circular cross-section thermal prediction (convection and radiation).*
- 2-D Heat Transfer with Cooling by Convection
  - *Spatial-varying cross-section thermal prediction (convection only).*
- 2-D Heat Transfer by Convection and Radiation
  - *Spatial-varying cross-section thermal prediction (convection and radiation).*
- 2-D Heat Transfer with Temperature-Dependent Conductivity
  - *Spatial-varying cross-section thermal prediction (convection, radiation, and temperature-dependent conductivity).*
- 2-D Heat Transfer in a Composite Section with Temperature-Dependent Conductivity
  - *Spatial-varying composite cross-section thermal prediction (convection, radiation, and temperature-dependent conductivity).*
- 2-D Axisymmetric Heat Transfer with Nonuniform Heat Flux
  - *Spatial-varying cross-section thermal prediction (convection, radiation, and nonuniform heat flux).*
- Lumped Mass with Moisture Evaporation.
  - *Simplified (0-D) general-purpose thermal prediction including latent heat effect.*
- 1-D Heat Transfer with Moisture Evaporation
  - *General-purpose thermal prediction including latent heat effect.*
- 2-D Heat Transfer with Moisture Evaporation
  - *Spatial-varying cross-section thermal prediction including latent heat effect.*
- 2-D Heat Transfer in a Composite Section with Moisture Evaporation and Temperature-Dependent Conductivity
  - *Spatial-varying composite cross-section thermal prediction (latent heat effect and temperature-dependent conductivity).*
- 2-D Heat Transfer in a Composite Section with Cavity Radiation

- *Spatial-varying composite cross section including cavity radiation.*

- 3-D Heat Transfer with Nonuniform Heat Flux
  - *General-purpose spatial-varying thermal prediction including nonuniform heat flux.*

Each example problem from the SFPE S.02 standard is material generic (*see Sect. 5.3 for thermal properties of specific construction and protective materials*) and has solved temperature history results. Hence, these example problems can be used to verify model/software predictions as well as adapt to specific materials and fire conditions. Also, these example problems have escalating levels of precision/complexity, the need for which will depend upon the specific structural fire engineering application.

5.3 Thermal Properties of Materials

The thermal properties of materials used in a heat transfer analysis govern the temperature gradients within the structural element. Therefore, it is key to assess thermal conditions as a function of the thermal properties of the material. The key thermal properties used for heat transfer analysis in structural fire engineering design include density, thermal conductivity, specific heat, and emissivity/absorptivity. In heat transfer analysis, it is usually assumed that absorptivity of materials is equal to their emissivity; hence, the term emissivity is used herein to reference both material properties.

5.3.1 Steel

Compared to other construction materials, steel has thermal properties that are very well established and relatively consistent among various sources. The key thermal properties of steel for use in structural fire engineering design include density, emissivity, thermal conductivity, and specific heat. Steel does not experience any appreciable latent heat effects at elevated temperatures.

The density of steel has a value of 7850 kg/m^3. This value does not appreciably change at elevated temperatures, and may be taken as constant.

The emissivity of steel varies depending upon aspects of its surface finish, including surface roughness, presence of oxidation, presence of galvanic coating, polishing, and/or presence of paint. Eurocode 3 specifies design values of 0.7 and 0.4 for carbon steel and stainless steel, respectively [10]. However, it should be noted that the emissivity of steel at ambient can range from 0.2 to 0.9 [13].

It is typical to assume that the emissivity of steel is constant with temperature. However, temperature-dependent expressions have been proposed, including the following [14]:

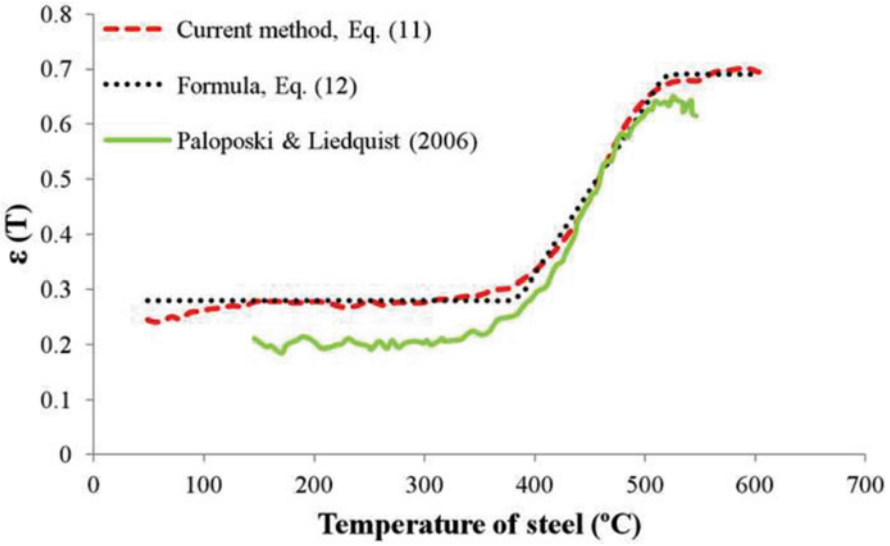

Fig. 5.7 Steel emissivity expression and test results [14]

For $T < 380^{\circ}\text{C}$, $\varepsilon = 0.28$
For $380^{\circ}\text{C} \leq T < 520^{\circ}\text{C}$, $\varepsilon = 0.00304T - 0.888$
For $520^{\circ}\text{C} \leq T$, $\varepsilon = 0.69$

Figure 5.7 plots the expression above along with test results obtained by Paloposki and Liedquist [15].

In addition to temperature dependence, the emissivity of steel may also vary depending upon the level of adhesion of soot to the surface during a fire. Except for extremely thin films, adhered soot has an emissivity of approximately 0.95 [16], which may be considered as constant. Hence, it may be prudent to consider a steel emissivity value toward the higher end of reported ranges if soot adherence is anticipated.

It is well known that steel is a very high conductor of heat. Eurocode 3 provides the following expression for the thermal conductivity of steel as a function of temperature [10]:

For $20^{\circ}\text{C} \leq T \leq 800^{\circ}\text{C}$, $k = 54 - 0.0333T$
For $800^{\circ}\text{C} < T \leq 1200^{\circ}\text{C}$, $k = 27.3$

Figure 5.8 plots the expression above.

The specific heat of steel remains relatively constant with temperature, except within a small-temperature bandwidth (between 700 °C and 800 °C) in which a pronounced metallurgical change occurs. Accounting for this metallurgical change, Eurocode 3 provides the following expression for the specific of steel as a function of temperature [10]:

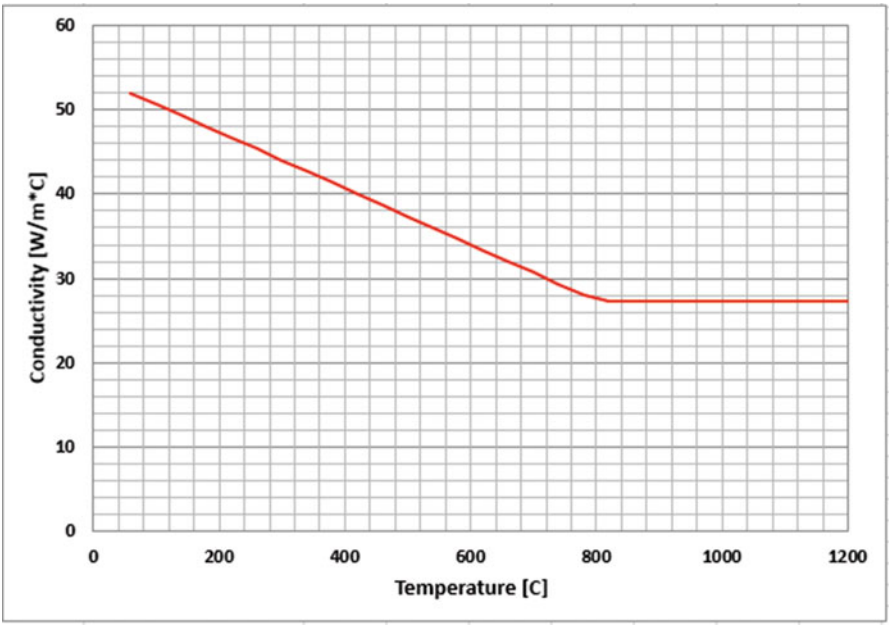

Fig. 5.8 Steel thermal conductivity

For $20^{\circ}\text{C} \leq T \leq 600^{\circ}\text{C}$, $c_p = 425 + 0.773T - 0.00169T^2 + 0.00000222T^3$
For $600^{\circ}\text{C} < T \leq 735^{o}\text{C}$, $c_p = 666 + 13002/(738 - T)$
For $735^{\circ}\text{C} < T \leq 900^{\circ}\text{C}$, $c_p = 545 + 17820/(T - 731)$
For $900^{\circ}\text{C} < T \leq 1200^{\circ}C$, $c_p = 650$

Figure 5.9 plots the expression above.

5.3.2 Concrete

The thermal properties of concrete depend upon the following inherent characteristics:

- Moisture content.
- Porosity.
- Density.
- Aggregate type.

Although moisture in concrete will evaporate to a certain extent under heating, it generally does not change considerably with temperature, and therefore can be treated as constant. Otherwise, the reduction in density due to free water loss and

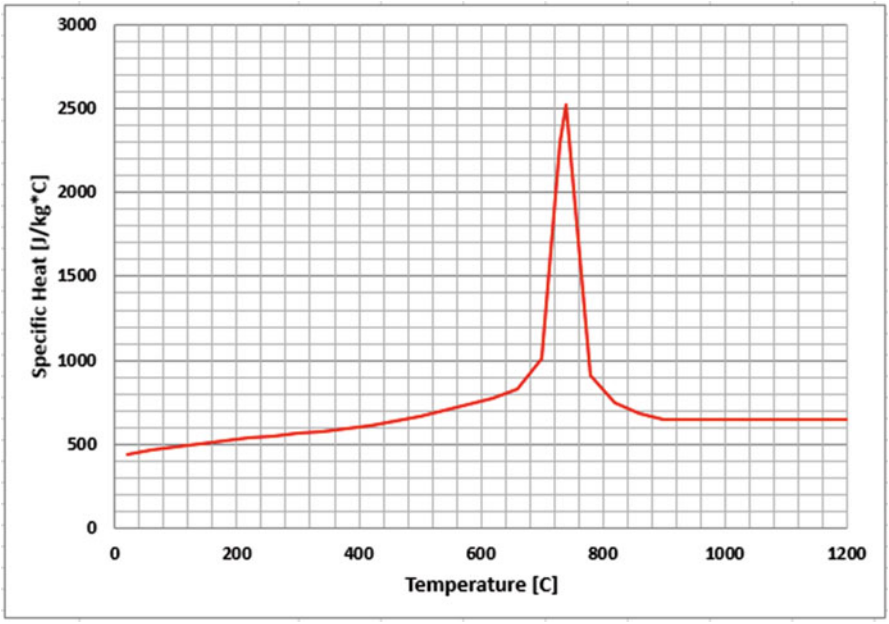

Fig. 5.9 Steel-specific heat

the density ρc (in kg/m^3) at temperature T (in Celsius) may be determined by the following equation [17]:

$$\rho_c = \begin{cases} \rho_{c,20} & \text{for } 20\ C \leq T \leq 115\ C \\ \rho_{c,20}[1 - 0.02(T - 115)/85] & \text{for } 115\ C < T \leq 200\ C \\ \rho_{c,20}[0.98 - 0.03(T - 200)/200] & \text{for } 200\ C < T \leq 400\ C \\ \rho_{c,20}[0.95 - 0.07(T - 400)/800] & \text{for } 400\ C < T \leq 1200\ C \end{cases}$$

where ρc,20 is the density of concrete at ambient temperature (in kg/m3).

Also from Eurocode 2, the thermal conductivity kc (in W/m-K) of normal-weight concrete at temperature T (in Celsius) can be determined between the upper and lower limits given in the following equations:

$$k_c = \begin{cases} 2 - 0.2451(T/100) + 0.0107(T/100)^2 & \textit{upper limit} \\ 1.36 - 0.136(T/100) + 0.0057(T/100)^2 & \textit{lower limit} \end{cases}$$

For most applications, the consideration of the upper limit thermal conductivity would yield conservative results.

For lightweight concrete with density between 1600 kg/m3 and 2000 kg/m3, the conductivity kc (in W/m-K) is given as [17]

$$k_c = \begin{cases} 1 - (T/1600) & for\ 20\ C \leq T \leq 800\ C \\ 0.5 & for\ 800\ C < T \leq 1200\ C \end{cases}$$

Per Eurocode 2, for normal-weight concrete, the specific heat of dry concrete Cc (in J/kg-K) at temperature T (in Celsius) is given as

$$c_c = \begin{cases} 900 & for\ 20\ C \leq T \leq 100\ C \\ 900 + (T - 100) & for\ 100\ C < T \leq 200\ C \\ 1000 + \dfrac{T - 200}{2} & for\ 200\ C < T \leq 400\ C \\ 1100 & for\ 400\ C < T \leq 1200\ C \end{cases}$$

When moisture content is not modeled explicitly, the specific heat of concrete c_c^* (in J/kg-K) can be considered for the following moisture content values (u) at 115 °C:

$$c_c^* = \begin{cases} 1470 & for\ u = 1.5\% \\ 2020 & for\ u = 3.0\% \\ 5600 & for\ u = 10.0\% \end{cases}$$

The parameter u is the moisture content. For lightweight concrete with density between 1600 kg/m^3 and 2000 kg/m^3, the specific heat is assumed to be independent of temperature and of magnitude 840 J/kg-K.

For normal-weight and lightweight concrete, the emissivity of concrete generally ranges between 0.85 and 0.95 [13].

5.3.3 Timber

Unlike steel and concrete, timber is a combustible material. As such, it undergoes thermal decomposition when exposed to fire, as illustrated in Fig. 5.10. The thermal decomposition of wood is governed by physical and chemical processes that transform the wood to char, a process that is known as *pyrolysis*. Some key features of the pyrolysis of wood include mass loss, discoloration, and emission of gaseous by-products [19]. Pyrolysis of wood is incredibly complex and depends on several factors including oxygen concentration, moisture content, and orientation of the specimen to the heat source [20]. In practice, the charring of timber usually occurs between 280 and 320 °C, with a temperature of 288 °C used to locate the pyrolysis front in wood specimens using embedded thermocouples [21].

The thermal analysis of wood must take into account the fact that the thermal decomposition of wood changes the physical properties of the material. Thus, heat

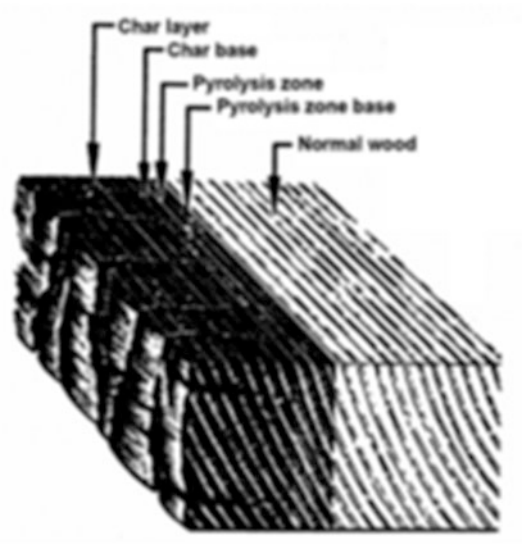

Fig. 5.10 Char layer and pyrolysis zone in wood [18]

transfer analysis of fire-exposed structures inevitably includes some level of modeling of the pyrolysis front, which is the transition zone between the virgin wood and the char layer (Fig. 5.10). A variety of simple and advanced calculation methods can be found in the literature.

It is important to note that, while pyrolysis is inherently a complex and nonlinear process, simplified models, such as the linear model in Eurocode 5 [22] or the nonlinear model in the National Design Specification [23], are based on a single parameter: the nominal char rate. The nominal char rate β_0 is defined as the char rate at 1 h of standard fire exposure. The nominal char rate depends on the species of wood (i.e., softwood versus hardwood), whether the member is solid-sawn wood or is a built-up member (e.g., glue-laminated timber), the moisture content of the wood, and the direction of heating (i.e., parallel to the grain versus perpendicular to the grain). Nominal char rates for various wood products can be found in the literature (e.g., FPL [24] and Eurocode 5).

Knowing the nominal char rate, the depth of the char layer can then be determined as a function of time. According to the linear model in Eurocode 5, for example, the depth of the char layer is given as

$$d_{char} = \beta_0 t$$

where t = time [min] and β_0 is the nominal char rate [mm/min]. Note that the equation above is a one-dimensional model. Additional factors (e.g., corner rounding) must be taken into account when a member is heated on more than one side.

In regard to the thermal properties (i.e., density, conductivity, and specific heat), it is recommended that temperature-dependent properties be obtained from

experimental tests, especially given the sensitivity of these properties to the wood species, the moisture content, etc. However, Annex B of Eurocode 5 provides design values that may be useful for some design applications.

5.3.4 Applied Passive Fire Protection

Where a structural or heat transfer assessment determines that a member requires the application of an applied passive fire protection material, there are a number of options available to a designer. A non-exhaustive list of insulating materials includes:

- Spray fire-resistive materials (SFRM).
- Intumescent coatings (or reactive coatings).
- Fire-rated board.
- Fire-rated blankets.
- Concrete encasement.
- Concrete filling.
- Timber.
- Water filling.

For each material, the principal remains the same. They work to restrict the transmission of heat to the underlying or associated substrate to ensure that it keeps sufficiently cool with the intent of maintaining stability in the event of a fire.

The choice of protective material is often dictated by architectural or constructional design considerations (e.g., durability or ease/speed of application). For example, for aesthetical reasons an intumescent coating (Fig. 5.11) may be preferential, while for cost reasons a SFRM material may be more appealing. Nonetheless,

Fig. 5.11 Shop application of an intumescent coating [Image courtesy of International Paint Ltd.]

the choice of material warrants careful consideration at the design and specification stages of a project.

All passive fire protection materials are subject to rigorous fire testing to and certification against a recognized standard. The choice of the appropriate testing, assessment, and certification requirement for the product will depend on the region or project location. For example, a project in Australia requires testing to AS 1530–4 and assessment to AS 4100. However, New Zealand typically accepts the BS 476–21 standard. Similarly there are different test standards that are required for mainland Europe, North America and Canada, Russia, China, etc. to which products need to be tested and assessed.

The following standards are typically referenced and requested for passive fire protection materials:

- BS 476 Parts 20–22 (historically common due to the influence of British Standards).
- EN 13381 Part 4 (passive materials) and Part 8 (reactive materials).
- ASTM E-119/UL 263 (North America-based codes).
- GB 14907 (Chinese fire test standard).
- GOST (Russia and Commonwealth of Independent States (CIS) region).

Manufacturers of proprietary passive fire protection materials are generally able to supply data relating to thickness for specific structural designs in relation to certified testing. Datasets like these are typically acceptable by authorities having jurisdiction.

For cases where a nonstandard design warrants further attention via an engineering study it may be beneficial to undertake either a heat transfer assessment or bespoke testing. The former is a common method but not all manufacturers will be able to provide a set of temperature-dependent material properties. Product data sheets may state values relating to density, specific heat capacity, and thermal conductivity but the designer should satisfy themselves that any such values are valid over the temperature range of interest and not just measured ambient values. Ideally, any such engineering assessment should reference back to available supporting test data where it is available to ensure a robust study.

5.4 Special Design Considerations

Although typically heat transfer analysis of structural elements is simplified under a range of possible assumptions, there are particular applications in which a more complex analysis is required in order to account for special design considerations.

5.4.1 Phase Change

In structural fire engineering, a phase change occurs when the temperature is high enough to cause a solid to transition into a liquid (i.e., melting) or a liquid to transition into a gas (i.e., evaporation). Temperatures associated with fires in buildings are generally not hot enough to cause melting of structural materials (e.g., steel, concrete, and timber). Some materials, like concrete and timber, however, do contain moisture, and it is important to note that the evaporation of moisture can directly affect the temperature in the structure.

From principals of thermodynamics, the amount of heat Q that is needed to cause a mass m to undergo a phase change from solid to liquid is given as

$$Q = mL_f$$

Similarly, the amount of heat Q that is needed to cause a mass m to undergo a phase change from liquid to gas is

$$Q = mL_v$$

Here, L_f = latent heat of fusion, and L_v = latent heat of vaporization. The latent heat of fusion and the latent heat of vaporization are properties that are unique to the specific material. Water, for example, has a latent heat of fusion L_f of 334 kJ/kg and a latent heat of vaporization of L_v is 2260 kJ/kg.

In conduction heat transfer, latent heat effects are added to the sensitive heat effects in the energy storage term of the heat conservation equation. Wickström [4] explains how to model latent heat effects associated with moisture evaporation in a solid using *specific volumetric enthalpy*. Wickström also derives an *effective* specific heat capacity that accounts for the latent heat effect. The effective specific heat results in a spike in the specific heat when temperature reaches the boiling point for water. The spike implicitly represents the energy storage associated with the phase change. It is important to note that the methods of using specific volumetric enthalpy and effective specific heat are equivalent, and both are suitable for structural fire engineering applications.

5.4.2 Insulation Mechanical Integrity

In the context of structural fire protection, mechanical integrity is defined as the ability of protective insulation to maintain its function under fire exposure. Changes in thermal properties at elevated temperatures are considered separately, for mechanical integrity primarily relates to the integrity of protective insulation. Accordingly, the following phenomena would represent mechanical integrity failures:

- Loss of adhesion (e.g., of SFRM) (Fig. 5.12).
- Loss of cohesion (e.g., of SFRM) (Fig. 5.13).
- Local damage (e.g., due to impact) (Fig. 5.14).
- Delamination (e.g., of gypsum wallboard layers) (Fig. 5.15).
- Loss of attachment (e.g., of gypsum wallboard layers).
- Spalling (e.g., of high-strength concrete) (Fig. 5.16).
- Other failures (e.g., degradation/disintegration of material).

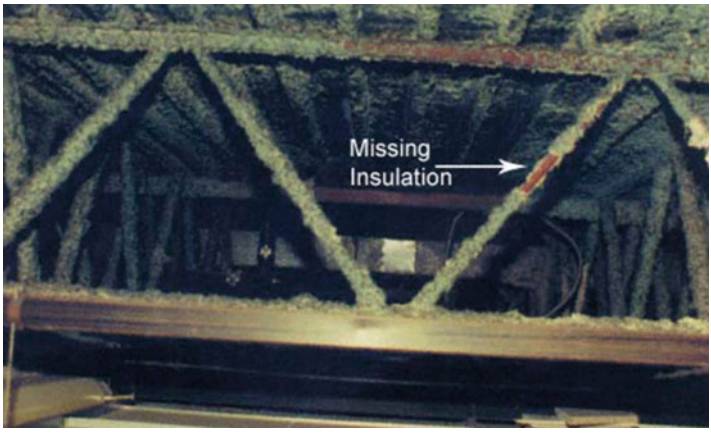

Fig. 5.12 SFRM adhesion failure (localized) [25]

Fig. 5.13 SFRM cohesion failure (during a pull test) [25]

Fig. 5.14 SFRM local damage due to impact [25]

Fig. 5.15 Gypsum wallboard delamination due to fire exposure [26]

The mechanical integrity of protective insulation under fire exposure cannot be reliably predicted using analytical tools. Heat transfer calculations inherently assume that protective insulation will remain in place during fire exposure. Accordingly, the designer should be confident that protective insulation will stay in place long enough to fulfill the required performance objectives.

Fig. 5.16 Reinforced concrete wall that experienced spalling [27]

The mechanical integrity of protective insulation under fire exposure remains a major knowledge gap/research frontier within structural fire engineering. Consequently, there is significant onus on the designer to derive appropriate empirical data and employ careful judgment based on this data and its applicability to the application.

The determination of adequate mechanical integrity of protective insulation is typically evaluated using standard fire testing within standard fire resistance design. However, standard fire testing does not adequately capture the effect of structural deformations on the mechanical integrity of protective insulation, which can be significant. For instance, large deflection of long-span beams under fire exposure may cause protective insulation to undergo adhesion failure, or gypsum board encasement systems to become unstable [25]. Standard fire testing does not inform the designer about these effects since realistic fire exposure and structural deformations are not simulated, and the supporting boundaries of the furnace apparatus do not undergo any deformation. Hence, addressing this concern requires the designer to develop specific performance criteria per the discretion of the building authority.

Fire resistance listings define appropriate extrapolations from test conditions, such as application to heavier steel sections than tested. However, dimensional scaling is usually not appropriate to qualify the mechanical integrity of protective insulation as part of a structural fire engineering design. For instance, the

endothermic calcination process that SFRM undergoes upon heating (which enhances its insulating capability) cannot be scaled based upon its thickness. Other examples include a very thin material that may not maintain its mechanical integrity, or an intumescent material that will yield little or no additional benefit if a thicker layer is applied. Hence, the use of protective insulation thicknesses that are outside the range included in specific fire resistance listings should not be done without validation testing or specific information from the manufacturer, as materials are often not as useful at thicknesses outside the range included in the testing.

Information derived from standard fire testing could be used to assist designers evaluating the anticipated level of mechanical integrity of protective insulation under fire exposure. At a minimum, the applicability of the standard furnace exposure to the structural design fires under consideration should be evaluated. Accordingly, the designer should exercise caution if a structural design fire is significantly more severe (e.g., sharper growth) as compared to the standard furnace test exposure. This may require the specification of applied insulation that has been qualified for challenging exposures (e.g., the UL 1709 exposure [28]).

In addition comparing structural design fires to test exposures, the designer may consult the relevant manufacturer for specific information, or refer to publicly available test data. At a minimum, the designer should adhere to the manufacturer's installation requirements (e.g., restrictions on the use of steel primers prior to the application of SFRM).

The industry has yet to develop a test method to qualify the mechanical integrity performance of protective insulation for nonstandard fire exposure and generalized application in structural fire engineering. Hence, it is currently within the purview of the designer to provide sufficient evidence, analysis, and judgement in this respect. This may require specific information from the relevant manufacturer. In this respect, the availability of information from relevant manufacturers is paramount, and perhaps indicative of their competitive advantage for inclusion in structural fire engineering applications.

References

1. ISO 834-11: Fire Resistance Tests—Elements of Building Construction, 2014.
2. EN 1991-1-2: Eurocode 1: Actions on structures—Part 1–2: General actions—Actions on structures exposed to fire, 2002.
3. SFPE S.01, Engineering Standard on Calculating Fire Exposures to Structures, Society of Fire Protection Engineers, Bethesda, MD, 2011.
4. Wickström, U. (2016). *Temperature calculation in fire safety engineering*. Springer.
5. Lattimer, B. Y. (2008). Heat fluxes from fires to surfaces. In Dinenno et al. (Eds.), *The SFPE Handbook of Fire Protection Engineering* (4th ed.). National Fire Protection Association.
6. Torero, J. L., Law, A., & Maluk, C. (2017). Defining the thermal boundary condition for protective structures in fire. *Structures, 149*, 104–112.
7. LaMalva, K. (2011). Thermal response of steel structures to fire: Test versus field conditions. *Journal of Fire Protection Engineering, 21*, 4.
8. Buchanan, A., & Abu, A. (2017). *Structural design for fire safety* (2nd ed.). John Wiley & Sons.

9. Eurocode 1: Actions on structures, Part 1–2: General actions—Actions on structures exposed to fire, Brussels, Belgium, European Committee on Standardization, 2002.
10. Eurocode 3: Design of steel structures: General rules—Structural fire design, Belgium, European Committee on Standardization, 1995.
11. Incroperia, F., DeWitt, D., Bergman, T., & Lavine, A. (2009). *Introduction to heat transfer*. Wiley.
12. SFPE S.02: Standard on calculation methods to predict the thermal performance of structural and fire resistive assemblies, Society of Fire Protection Engineers, 2015.
13. FABIG, Fire Resistant Design of Offshore Topside Structures, Fire and Blast Information Group, Technical Note No. 1, The Steel Construction Institute, Berkshire, UK, 1993.
14. Sadiq, H., Wong, M., Tashan, J., Al-Mahaidi, R., Zhao, X.. Determination of steel emissivity for the temperature prediction of structural steel members in fire, 2013.
15. Paloposki, T., Liedquist, L. (2005). Steel emissivity at high temperatures, Report VTT-TIED-2299, VTT Technical Research Centre of Finland
16. Libert, C., Hibbard, R. (1970). Spectral emittance of soot, NASA Technical Note D-5647, National Aeronautics and Space Administration, Washington, D.C.
17. Eurocode 2: Design of concrete structures—Part 1–2: General rules—Structural fire design, EN 1992-1-2: 2004.
18. Schaffer, E.L. (1967). Charring Rate of Selected Woods-Transverse to Grain. Res. Pap. FPL 69. Madison, WI: USDA Forest Service, Forest Products Laboratory.
19. Buchanan, A. (2002). *Structural design for fire safety*. John Wiley & Sons, Ltd..
20. Moghtaderi, B. (2006). The state-of-the-art in pyrolysis modelling of lignocellulosic solid fuels, fire and materials, No. 30.
21. Schaffer, E. (1984). *Structural fire design: Wood, Forest Products Laboratory Research Paper FPL 450*. USDA Forest Service.
22. EN 1995-1-2: Eurocode 5: Design of timber structures—Part 1–2: General—Structural fire design, 2004.
23. AWC. (2012). *National design specification (NDS) for wood construction*. American Wood Council.
24. FPL, Wood Handbook: Wood as an Engineering Material, Forest Products Laboratory General Technical Report FPL-GTR-190, USDA Forest Service, Madison, WI, 2010.
25. Carino, N., et al. (2005). *NIST NCSTAR 1-6A passive fire protection, federal building and fire safety investigation of the world trade center disaster*. National Institute of Standards and Technology.
26. TFRI Fire Test of Wood Frame Assembly, European Wood, Brussels, Belgium, http://jp.europeanwood.org, 2017.
27. Jansson, R. (2013). *Fire spalling of concrete: Theoretical and experimental studies, doctoral thesis in concrete structures*. KTH Royal Institute of Technology.
28. UL 1709: Standard for rapid rise fire tests of protection materials for structural steel, Underwriters Laboratories, Northbrook, IL, 2011.